Diyala Journal of Engineering Sciences

Journal homepage: https://djes.info/index.php/djes

ISSN: 1999-8716 (Print); 2616-6909 (Online)

Photovoltaic MPPT Control Strategy Based on Tuna Swarm Optimization TSO Algorithm

Zeyad Assi Obaid, Ali Sachit Kaittan*, Hassan Jasim Mohammed

Department of Electrical Power and Machines Engineering, University of Diyala, 32001 Diyala, Iraq

ARTICLE INFO

Article history:
Received: 26/10/2025.
Revised: 04/07/2026.
Accepted: 18/07/2026.
Available online: 15/09/2026.

Keywords:
MPPT
Tuna Swarm Optimization
Partial Shading
Photovoltaic Systems
Hybrid Algorithm

ABSTRACT

In photovoltaic systems, multiple power peaks imitated by the partial shading led to trapping of conventional maximum power point tracking MPPT algorithms such as Perturb and Observe (P&O) at local maxima resulting in about 30–50% power loss. A hybrid Tuna Swarm Optimization-Perturb and Observe (TSO-P&O) algorithm is proposed in this paper where the location of global maximum power point (MPP) estimated by using TSO and local refinement provided through P&O based on a sudden change from environmental with an adaptive restart mechanism. TSO-P&O outperforms P&O, Particle Swarm Optimization (PSO), Genetic Algorithm (GA) and Grey Wolf Optimizer (GWO) validated by MATLAB/Simulink. It reaches a maximum static shading efficiency of 99.06% and dynamic shading convergence in as fast as 0.071s (98.52%) with the same equipment, respectively; It also displays a minimized steady-state oscillation (0.42% standard deviation) and superior statistical performance at $p < 0.05$ as well. The algorithm is very suitable for real-time embedded implementation, with a runtime of 2.5 ms per iteration and a memory footprint of only 5 KB. Experimental validation of the proposed algorithm against a hardware-prototype, extension to larger PV arrays experiencing more complex shading patterns, and hybridizations with learning-based methods could yield additional opportunities for enhanced performance in future work.

1. INTRODUCTION

With the continuous development and progress of society, human beings' demand for various types of energy is increasing, resulting in a constant decline in traditional fossil fuels. According to relevant statistics, at the current rate of human energy consumption, the Earth's oil reserves will be depleted within 50 years, and natural gas and coal can only sustain human use for approximately 120 years [1]. In addition, the large-scale use of traditional fossil energy will not only exacerbate the world's energy crisis but also cause significant pollution to the ecological environment. Based on the above factors, Fan et al. [2] show that accelerating the safe and efficient use of new, clean, and sustainable energy has become a challenge that humans must face. Photovoltaic power generation (PV) is the most effective way to utilize solar energy.

For photovoltaic power generation systems, Balachandran and Ramasamy [3] and Wang et al. [4] conclude that the output power is easily affected by environmental factors and under certain environmental conditions, the photovoltaic system produces maximum power at a specific working voltage or working current. They also named the Maximum Power Point Tracking (MPPT) as the key measure to enable the photovoltaic system to output maximum power and improve efficiency. The MPPT algorithm has therefore become the focus of photovoltaic research worldwide.

Atia et al. [5] and Li et al. [6] approved that under uniform illumination, the PV array's P-U curve exhibits a single peak, and traditional MPPT algorithms such as Perturb and Observe (P&O) and Incremental Conductance (INC) perform effectively. But, if the PV array is locally shaded, its P-U curve will give multiple peaks. In this matter, MPPT algorithms based on local peak power points tracking are usually not efficient because of searching a local maximum point instead of the global maximum power point (GMPP), which would have resulted in lost power amounts ranging from 30 to 50%.

The partial shading problem has been the subject of significant research efforts. Metaheuristic algorithms for MPPT control, like Particle Swarm Optimization (PSO) [7–8], Genetic Algorithm (GA) [9], Grey Wolf

*Corresponding author's E-mail: alisachit@uodiyala.edu.iq | ORCID: 0000-0003-1799-5289
DOI: 10.24237/djes.2026.19305

Optimizer (GWO) [10] and Ant Colony Optimization (ACO) [11]. However, they are limited by early searching attracted to local optima, slow convergence speed in dynamic situations, considerable and persistent steady-state oscillation, and a large sensitivity towards multiple parameters.

Xie et al. [12] recently proposed a new metaheuristic algorithm called the Tuna Swarm Optimization (TSO) algorithm which is based on fish and specifically mimics tuna school cooperative foraging tendency. TSO uses one of the two distinct foraging procedures (spiral or parabolic) to properly analyze difficult hunting areas without reducing convergence rate. Compared to other metaheuristics, TSO has many advantages such as:

(1) balancing the exploration-exploitation mechanism which decreases premature convergence risk.

(2) carrying fewer control parameters in making implementation and tuning easier than population-based algorithms.

(3) using an adaptive weight coefficient modulating the strength of search behavior dynamically.

Yet, little work has been done on the use of TSO on PV MPPT under partial shading despite these benefits. Quite a few research works in TSO-based DP MPPT domain can be found. Though preliminary work on these techniques Wang and Chang [13] and Li et al [14] has produced promising results, they also have significant limitations: implementation is limited to only CV-based sequential switching between TSO and P&O with no adaptive logic; validation is confined to static shading cases; comparison is limited exclusively against P&O; full reporting of parameters in sufficient detail for reproducibility (including location information) is lacking.

This paper identifies these gaps and proposes a novel combined MPPT algorithm in which TSO integrates with P&O in an adaptive framework. The key contributions of this work are as follows:

(1) New hybrid MPPT algorithm; TSOP (dynamic switching mechanism based on convergence criterion + adaptive TSO-P&O approach that integrates TSO global search ability and P&O local fine-tuning with some uses of a stationary-converter-only level hill climbing, as a generalization method to adaptive restart condition for environmental situation change.

(2) Validation; Analytical—Extensive MATLAB/Simulink based simulations in static and dynamic partial shading conditions with comprehensive comparatives against P&O, PSO, GA and GWO.

(3) Transparency for parameters; Full reporting on all TSO parameters, shading scenarios, simulation setup and statistics from 30 independent runs to allow verification.

(4) Performance: Faster convergence (0.07s versus 0.1s), Higher efficiency (99.06% versus 95.16%), Lower power oscillation against original one.

The remaining content of this paper is structured as follows. In Section 2 we review many of the current state-of-the-art methods for MPPT and in section 3 follows our mathematical model of a photovoltaic cells. Section 4 focuses on the principle of MPPT control. We do a description of the P&O method in Section 5. Section 6 contains the introduction of the TSO algorithm and also explanations for this proposed hybrid MPPT approach: called as TSOP&O. Section 7 presents the analysis and simulation results. Section 8 concludes the paper.

2. LITERATURE REVIEW

2.1 Classical MPPT Methods

Traditional MPPT Algorithms includes Constant Voltage Method, Incremental Conductance Method and Perturbation and Observation method. Katche et al. [15], Shams et al. [16], and Zhu et al. [17] discussed and developed an intelligent algorithm to locate the maximum power point rapidly these methods. The simplicity of these methods and implementation process makes them different. But they are slower, and their tracking is poor.

Pendem et al. [18] optimized the perturbation step size of P&O to make it more accurate and faster. To solve the response speed and output power oscillation problem of incremental conductance technique, M. Awan and F. Awan [19] proposed new step-size modification methods. For standalone solar PV systems, it is possible to use advanced algorithms such as (Decrease and Fix) based approaches on the Perturb and Observe (P&O) algorithm to achieve a faster tracking speed while mitigating oscillations around the maximum power point.

Belhimer et al. [20] developed a standalone PV system with an MPPT algorithm for the design of a quadratic boost converter. The proposed topology is controlled by hard-switching signal based PWM with a variable duty-cycle dictated given through the MPPT algorithm.

It can be concluded from Prajapati and Fernandez [21], Mohamed et al. [22], and Worku et al. [23] that the main drawback of classical MPPT strategies is that they assume a single-peak P-U curve when the generation condition changes. These techniques are often failed out due to landing on local maxima because the partial shading result would produce multiple peaks.

Zhang et al. [24] proposed a modified hybrid PSO-P&O MPPT algorithm with an innovative method of initial particle positioning to minimize the number of particles and bypass local maxima. internally, was employed to accelerate convergence and a reinitialization procedure allowed the algorithm to complete retrack in face of instantaneous as well as slow light intensity variations.

2.2 Metaheuristic-Based MPPT Methods

Because classical methods are defective under partial shading in multi-panel systems, scientists have proposed to introduce a variety of metaheuristic algorithms into MPPT control.

Demirci et al. [25] proposed an improved artificial neural network (ANN)-based MPPT algorithm that is trained based on a diverse dataset, covering many shading conditions and different irradiation levels as well climatological condition with the metaheuristic algorithms are pivotal for improving training methods.
Guo et al. [26] presented a power switching control approach based on an innovative switched model for the Boost-based wind power MPPT system, which achieves precise representation of converter working process and allows direct power switching control without using PWM block.
Padmanaban et al. [27] suggested a principle with reference base on the improved Basil or Beetle Antennae Search (BAS) Algorithm performance for better output in connection to power maximum point tracking through double-stage three-phase solar grid integrated system.
Mao et al. [28] proposed a newly modified artificial fish swarm algorithm (MAFSA) as an MPPT method operated by the boost DC/DC converter. This method speeds up and accurately finds the maximum power point. With a connected ANPC inverter, the total system efficiency is improved for partial shading scenarios compared to classical PSO-based MPPT methods
De Oliveira et al. [29] utilized Genetic Algorithms (GA) to make sure the system works in partial shading conditions by reaching a global maximum point with GA approach and gaining the most possible power from PV configurations. Simulations were performed to compare the proposed strategy with the conventional P&O method, and it was proved that better power generation performance has been obtained by tracking process.
A hybrid Elephant Herding Optimization with Artificial Neural Network (EHO-ANN) for MPPT proposed by Vijayakumar and Govindaraju [30] in grid connected PV systems. The EHO algorithm stimulates clan potential around the global MPP, and an adapted Luo chopper with PID controller is employed to improve system performance in a wide range of solar irradiance and temperature changes. Their approach is novel as it combines meta-heuristic optimization together with AI techniques validated through both Matlab/Simulink and experimental setup.
Based on PSO-based approaches, the implementations of MPPT methods have been extensively engaged by the researchers. Imtiaz et al. [31] used PSO for maximum power point tracking, but the particles were initialized at voltages that correspond to peak points and thus increasing its ability of being stuck in local optima. Mah et al. [32] proposed a territory particle swarm algorithm based on the composition of a PSO procedure for fast tracking GMPP. More specifically, these improvements are achieved by employing a hybrid technique involving genetic algorithms along with concepts originating from ant colony optimization.
Nevertheless, metaheuristic-based MPPT approaches are still susceptible dealing with a few critical and long-standing complications:
(1) This leads to premature convergence; under complicated partial shading pattern, several algorithms will converge to local optimums.
(2) Poor speed of convergence; convergence times can be excessive under dynamic shading changes.
(3) Continuous oscillating; large power oscillating around the MPP and lead to reduce system efficiency.
(4) Parameter sensitivity: they are heavily dependent on parameter tuning and can depend highly from problem to problem.

2.3 Comparative Analysis of Existing MPPT Methods

To clearly position the proposed TSO-P&O method within the existing literature, Table 1 provides a structured comparison of representative MPPT approaches under partial shading conditions.

Table 1. Comparison of existing MPPT methods for partial shading conditions

Method	Category	Convergence Speed	Tracking Accuracy	Complexity	Partial Shading Suitability	Key Limitations
P&O [6]	Classical	Slow	Low	Low	Poor	Fails under multi-peak conditions
PSO [8]	Metaheuristic	Medium	High	Medium	Good	Premature convergence, parameter tuning
INC [5]	Classical	Medium	Medium	Medium	Poor	Fails under multi-peak conditions
GA [9]	Metaheuristic	Slow	High	High	Good	Computationally intensive
GWO [10]	Metaheuristic	Fast	High	Medium	Good	May converge prematurely
BFO [7]	Metaheuristic	Slow	Medium	Medium	Fair	Slow convergence
ANN [25]	Learning-based	Fast	High	High	Good	Requires extensive training data
Fuzzy Logic [21]	Learning-based	Fast	Medium	Medium	Fair	Rule-based, limited generalization

Hybrid PSO-P&O [24]	Hybrid	Medium	High	Medium	Good	Switching logic may be suboptimal
TSO-P&O (Proposed)	Hybrid	Fast	High	Medium	Excellent	Requires parameter selection

Research Gap and Motivation

The critical synthesis in the above section allows us to identify the following research gaps:

1- Static Partial Shading Validation Only: Existing studies are mostly limited to validation of the corresponding algorithm under static partial shading and very few evaluates performance when irradiance changes.

2- Poor comparative assessment: Lots of studies fell short as most compared only against P&O and those that did benchmark to common-used metaheuristics like PSO and GA, examined them under very different conditions.

3- Reported parameters do not specify full parameterization details: does not specify if entire spectrum of output data was used or even state a valid population to draw from during simulations, making it difficult for other investigators to reproduce what output parameters were modelled.

4- Suboptimal hybridization strategies: TSO based MPPT methods with limited validation are using simple sequential switching logic without any adaptive logic.

In that respect, this paper presents an adaptive TSO-P&O hybrid MPPT algorithm with extensive verification and parameter reporting, as well as rigorous comparator analysis against many established methods.

3. MATHEMATICAL MODEL OF PHOTOVOLTAIC CELLS

The equivalent circuit of a photovoltaic panel can be simplified to the structure shown in Figure 1. It mainly includes the photovoltaic cell's current output.

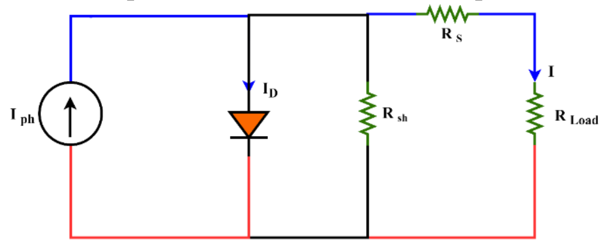

Figure 1. Equivalent circuit diagram of a PV panel

The figure simplifies it into a current source, a parallel diode, a parallel resistor R_{sh}, a series resistor R_s, and a load resistor R_L. R_{sh} mainly includes surface resistance, contact resistance, and body resistance. The series resistor R_s is primarily caused by dirt or impurities in the photovoltaic cell itself. I_{ph} is the current generated by the photovoltaic cell due to light, which is mainly affected by light intensity, temperature, and the structure of the photovoltaic cell itself. I_D is the current flowing through the parallel diode. It is precisely because of the existence of the parallel diode that the maximum power point of the photovoltaic output is not unique when multiple photovoltaic panels are used in parallel.

For photovoltaic cell circuits, the actual output current *I* of the photovoltaic cell can be analyzed using circuit principles as shown in formula (1).

$$I = I_{ph} - I_o[e^{q(\frac{U+IR_s}{AKT})} - 1] - [\frac{U+IR_s}{R_{sh}}] \tag{1}$$

Among them, I_o is the opposite saturation current of the parallel diode, U is the actual output voltage of the photovoltaic cell, A is the P-N junction coefficient of the semiconductor device in the photovoltaic cell, k is the Boltzmann constant, generally taken as 1.38×10-23J/K, and T is the ambient temperature. In addition, some assumptions made in the photovoltaic cell model: firstly, since the series resistance R_s is relatively small, usually less than 1 ohm, and the parallel resistance R_{sh} is relatively large, about 1 to 10 kiloohms, the current flowing through the parallel resistance part can generally be ignored; secondly, The series resistance R_s is retained in the model as it significantly affects the I-V curve's slope near the maximum power point; and finally, under partial shading and temperature variation, the model remains accurate because the diode saturation current I_o and photo-generated current I_{ph} are temperature-dependent and are updated in the simulation environment.

So, the actual output current *I* of the photovoltaic cell is corrected as shown in formula (2).

$$I = I_{ph} - I_o[e^{q(\frac{U+IR_s}{AKT})} - 1] \tag{2}$$

Therefore, by combining formula (2) with the power calculation formula, the output power *P* of the photovoltaic cell can be obtained as shown in formula (3).

$$P = I_{ph} * U - I_o * U * [e^{q(\frac{U+IR_s}{AKT})} - 1] \tag{3}$$

It can be seen from formula (3) that the output power of photovoltaic cells is primarily influenced by light intensity, temperature, and other internal factors, and changes nonlinearly in response to these factors [33-36].

4. MPPT CONTROL PRINCIPLE

As described in the previous section, the maximum power point output of photovoltaic arrays is prejudiced by various factors; however, the external environmental factors that have the most significant impact on their maximum power point are primarily light intensity and temperature. It is precisely because the maximum power point of photovoltaic cells changes with environmental changes that the MPPT control technology is critical in enabling the photovoltaic cells to operate at maximum working efficiency. There are currently two primary circuit connection forms for photovoltaic grid-connected systems: single-stage and double-stage. In the single-stage photovoltaic grid-connected system, the photovoltaic cells are directly linked to the DC side voltage bus of the grid-connected inverter, and the inverter generally undertakes its MPPT control. However, its PV controllable input range is narrow, so it is generally suitable for high-voltage grid-connected systems. In contrast, the double-stage photovoltaic grid-connected system also incorporates a DC/DC converter between the photovoltaic cell and the inverter, which undertakes the task of photovoltaic maximum power point tracking. Its adjustment range is broad, allowing it to be applied to various voltage grid-connected systems. This article mainly trains the double-stage grid-connected system. Taking the photovoltaic system based on a Boost converter as an example, its MPPT control principal circuit illustration is demonstrated in Figure 2.

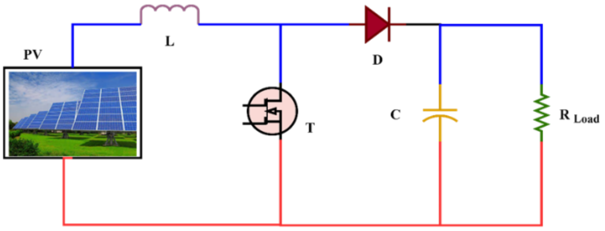

Figure 2. Circuit diagram of a photovoltaic system with a Boost converter for MPPT control.

From the circuit principle, we know that for a linear circuit, when the load impedance of the outside circuit and the internal impedance of the power supply reach a specific conjugate matching condition, the external circuit load can operate in its maximum power state.
For the photovoltaic grid-connected system, although it is practiced, the photovoltaic arrays and the DC/DC conversion circuit both operate in a nonlinear state; it is possible to make a reasonable assumption for a short time and regard them as a linear circuit system. Therefore, based on the above analysis, when the external impedance meets the conditions specified in formula (4), the photovoltaic arrays is in its maximum power output state.

$$R_L = R_{pv}\ ,\ P_{\max} = \frac{U_{pv}^2}{4R_L} \tag{4}$$

Where R_L: load resistor, R_{pv}: Equivalent resistance of the PV array. To achieve impedance matching, the duty cycle D of the DC/DC conversion circuit can be adjusted. The specific calculation is as follows. The association between the PV array output voltage U_{PV} and the Boost circuit output voltage U_{DC} can be expressed by formula (5).

$$\frac{U_{DC}}{U_{pv}} = \frac{1}{1-D} \tag{5}$$

For the convenience of analysis, the power loss inside the Boost circuit is ignored, so the relationship between the PV array output current, I_{PV}, and the Boost circuit output current, I_{DC}, can be expressed by formula (6).

$$\frac{I_{pv}}{I_{DC}} = \frac{1}{1-D} \tag{6}$$

Therefore, the resistance of the equivalent load R_L connected to the photovoltaic array is as shown in formula (7).

$$R_L = \frac{U_{DC}}{U_{pv}} = \frac{U_o(1-D)}{\dfrac{I_o}{1-D}} = R_o * (1-D)^2 \tag{7}$$

Where: U_o is the output voltage across the load, I_o is the output current through the load, R_o is the actual load resistance, D is the duty cycle of the Boost converter switch.
The voltage and current control are achieved through duty cycle adjustment of the Boost converter. The relationship between output voltage, input voltage, and duty cycle was given by equation (5) By modulating the duty cycle, the equivalent load impedance seen by the PV array is altered to match the optimal operating point. The MPPT algorithm changes the duty cycle to keep the energy produced by the PV array maximal whatever happens with load ones under variable load. Therefore, the TSO-P&O algorithm can be updated accordingly to previous load changes since when power deviation is larger than a threshold value because of any change in loads, the restart condition formula (7) will invoke another global search [37-39].

5. MPPT CONTROL METHOD BASED ON P&O

The P&O method is also commonly referred to as the hill-climbing method. This scheme is commonly utilized due to its simple hardware and software design, as well as the relatively few parameters required for measurement. For the P&O method, its basic principle is first to make a slight disturbance to the system, then observe the power output of the system, and compare the observation result with the previous state. Finally, the direction of the next disturbance is determined based on the comparison result. If the power output of the system increases relative to the previous state after the current disturbance, the next disturbance direction is the same as the current disturbance. Otherwise, the disturbance is applied in the opposite direction. This is the reason for the name of this method. As shown in Figure 3, the basic operating principle is as follows: First, the photovoltaic system is operated at a certain voltage, U_k. The output voltage and current of the photovoltaic power generation system are sampled through the sampling circuit, and the output power, P_k, at this time is calculated. Then, a positive perturbation, *ΔU*, is applied to the operating voltage of the photovoltaic power generation system, causing it to operate below a new reference voltage ($U_k = \Delta U$), and the output power, P_{k-1}, at this time is measured. If the output power, P_{k-1}, after the perturbation is greater than the output power, *P*, before the perturbation, it designates that the current operating point is to the left of the MPP, and the perturbation should continue in the same direction. If the output power, P_{k-1}, after the perturbation is less than the output power, P_k, before the perturbation, it indicates that the current operating point is to the right of the maximum power point, and the perturbation should be applied in the opposite direction at the next moment. By continuously perturbing the operating voltage of the photovoltaic system, the output power of the photovoltaic power generation system continuously approaches the MPP, eventually oscillating repeatedly at the MPP, thus achieving dynamic equilibrium.

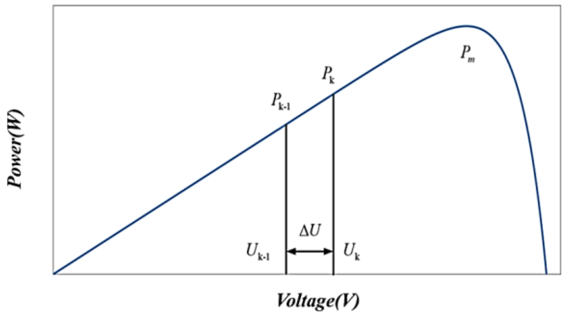

Figure 3. Schematic diagram of the P&O method

The specific process of the MPPT control scheme created on the P&O algorithm is illustrated in Figure 4. Although this method can effectively MPPT of the system, if the perturbation step size of this method is a fixed value, it is impossible to ensure both tracking accuracy and speed. Therefore, to solve this problem, the paper considers taking the difference between the output power of the current state and the output power of the previous state as a variable step size factor. At this time, if the difference between the two powers is significant, the perturbation step size will also be large. Conversely, the step size will be reduced. Once the power of the two states changes to zero, the system will be in a stable power output state until the photovoltaic cell is detected to change again. The process will continue. This method is straightforward and does not introduce new measurement variables into the system [40-41].

6. MPPT CONTROL METHOD WITH TSO ALGORITHM

6.1. Principles of Tuna School Optimization Algorithm

TSO's parabolic and spiral foraging strategies enable a more even search than PSO's single velocity-update mechanism. However, TSO− which uses adaptive weight coefficient to benefit from them — is more robust than WOA in this regard, since all the designs of weights keep CoE unsaturated by avoiding premature convergence due to the elimination of sub-optimal solutions. Compared to EHO and SSA, TSO is more robust due to the fewer number of sensitive parameters involved.

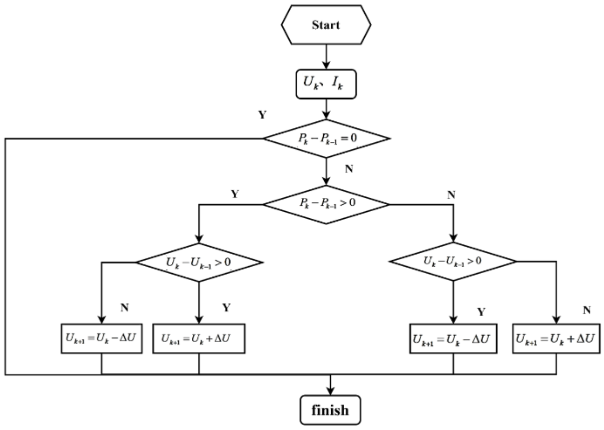

Figure 4. Flowchart of MPPT control scheme created on P & O

Tuna School Optimization is a population-based global optimization metaheuristic method. The TSO algorithm mimics the foraging patterns of two tuna schools. The foraging (optimization) process is characterized as follows: The first technique involves spiral foraging. When tuna schools forage, they swim in a spiral pattern to draw fish to shallow water; the second approach is a parabolic one. Each tuna swims behind the preceding fish's tail, creating a parabolic curve that surrounds the prey. Global optimization is accomplished using two foraging techniques. The mathematical equation for the spiral foraging technique is as described below:

$$A_i^{t+1} = a_1(A_{best}^t + \delta\left|A_{best}^t - A_i^t\right|) + a_2 * A_i^t, i = 1,2,3,4....,n \tag{8}$$

$$a_1 = a + (1-a) * \frac{t}{t_{\max}} \tag{9}$$

$$a_2 = (1-a) * (1 - \frac{t}{t_{\max}}) \tag{10}$$

$$\delta = e^{bx} * \cos(2\pi b) \tag{11}$$

$$x = e^{[3\cos\{(\frac{t_{\max}+1}{t-1})\pi\}]} \tag{12}$$

Where: A_i^{t+1} is the i^{th} discrete in the t+1th iteration; A_{best}^t is the best discrete in the current population, i.e., the food location; α_1 is the weight coefficient controlling the current discrete to move with respect to the previous discrete. *a*: is a constant used to limit the tendency of the individual to follow the best individual and the preceding discrete; *b*: is a random number between 0 and 1; *t* is the current iteration number, and $t_{\max}$ is the maximum iteration number.

When the optimal discrete cannot be realized (global optimality), mindlessly following the optimum discrete is not conducive to setting foraging. Therefore, producing random synchronies in the exploration space as orientation points for spiral foraging is conducive to escaping local optimality and enabling the algorithm to achieve global optimization capabilities. As shown in the following formula:

$$A_i^{t+1} = a_1(A_{rand}^t + \delta\left|A_{rand}^t - A_i^t\right|) + a_2 * A_i^t, i = 1,2,3,4....,n \quad (13)$$

Where A_{rand}^t : is a randomly produced orientation point in the exploration space. As the number of iterations increases, the tuna optimization algorithm should gradually transition from a global search to a precise local search. Therefore, as the number of iterations grows, the orientation point of the above tuna group in spiral foraging conversions from a random discrete to an optimal discrete. In rapid, the ultimate numerical model of the spiral foraging approach is as shown in formula (14):

$$A_i^{t+1} = \begin{cases} a_1(A_{rand}^t + \delta\left|A_{rand}^t - A_i^t\right|) + a_2 * A_i^t, i = 1,2,3,4....,n, rand < \dfrac{t}{t_{\max}} \\ a_1(A_{best}^t + \delta\left|A_{best}^t - A_i^t\right|) + a_2 * A_i^t, i = 1,2,3,4....,n, rand \geq \dfrac{t}{t_{\max}} \end{cases} \quad (14)$$

In addition to foraging in a spiral structure, tuna also form a parabola shape to hunt. Tuna uses food as a reference point to create a parabola foraging pattern. The detailed numerical model is as observed:

$$A_i^{t+1} = A_{best}^t + rand(A_{best}^t - A_i^t) + tf * p^2 * (A_{best}^t - A_i^t) \quad (15)$$

Where: tf is a random number, taking the value of 1 or -1.

In rapid, the mathematical expression of the tuna scavenging mathematical model can be summarized as formula (16):

$$A_i^{t+1} = \begin{cases} a_1(A_{rand}^t + \delta\left|A_{rand}^t - A_i^t\right|) + a_2 * A_i^t, i = 1,2,3,4....,n, rand < \dfrac{t}{t_{\max}}, \ rand > 0.5 \\ a_1(A_{best}^t + \delta\left|A_{best}^t - A_i^t\right|) + a_2 * A_i^t, i = 1,2,3,4....,n, rand \geq \dfrac{t}{t_{\max}} \\ A_{best}^t + rand(A_{best}^t - A_i^t) + tf * p^2 * (A_{best}^t - A_i^t), \ rand \leq 0.5 \end{cases} \quad (16)$$

Tuna schools approach prey through two foraging methods, each with a 50% chance of success. Through the iterative process, the optimal individual position is continuously updated, and the food is continually approached until it is finally captured [42-44].

6.2. Maximum power tracking of the TSO algorithm

The initial tuna school position can be randomly generated or placed as required. The initial population position has a particular relationship with the number of iterations. The appropriate selection can reduce the number of iterations, thereby reducing the convergence time. From the constant voltage method, it can be seen that the voltage corresponding to the maximum power point is generally 0.8 times the open-circuit voltage; however, this is not the case in the presence of partial shadows. Therefore, the initial population should be evenly distributed in the search space to ensure richness. For photovoltaic maximum power tracking, the aim function is the real-time output of the photovoltaic array, as shown in formula (17):

$$P = U * I \quad (17)$$

The value of the objective function power corresponds to the optimal individual and the position of food in the tuna school (duty cycle). The maximum value of the aim function power indicates that food has been found (optimal duty cycle).

After setting the initial population, the current population position is calculated, which involves determining the power corresponding to the duty cycle, and the optimal individual is then selected. Each population has a 50% probability of foraging, according to the mathematical formulas for spiral foraging and parabolic foraging, which is equivalent to iteration. During the spiral foraging process, a random number will be generated and compared with t/t_{max}, allowing the population to continue converging to the optimal individual and gather at the maximum power point.

The termination condition of the TSO approach in this paper is that when the iteration influences the set maximum number of iterations, the optimal individual location in the iteration process, that is, the optimal duty cycle, is output, and the iteration ends; if the maximum number of iterations is not reached, the iteration process is returned to continue iterating.

Since the shadow in the natural environment is not constant, the TSO algorithm can still perform MPPT after the shadow changes. The restart condition is set as shown in formula (18) to make the system restorable.

$$\frac{P_{now} - P_{old}}{P_{old}} > \Delta_{tv} \quad (18)$$

Where: P_{now} is the output power of the photovoltaic array currently detected; P_{old} is the max power in the previous iteration; Δ_{tv} is the pre-set threshold. The tuna school optimization procedure method is displayed in Figure 5 [45-46].

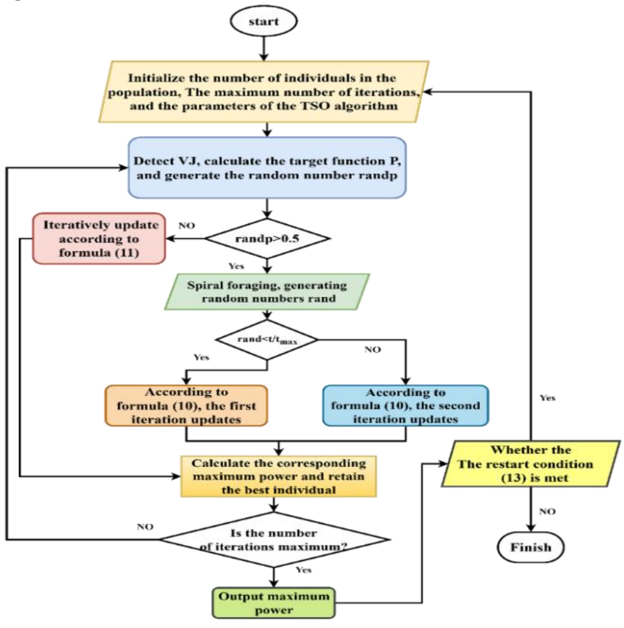

Figure 5. Flow chart of TSO

6.3 TSO Parameter Selection and Justification

The performance of the TSO algorithm depends on the appropriate selection of its hyperparameters. Based on preliminary sensitivity analysis and empirical testing, the parameters listed in Table 2 were selected for this study.

Table 2. TSO algorithm parameters

Parameter	Symbol	Value	Justification
Population size	N	20	Balanced between search diversity and computational cost; increasing beyond 20 yields <0.5% improvement in accuracy but increases computation by 30%
Maximum iterations	t_{max}	50	Sufficient for convergence based on preliminary analysis; algorithm stabilizes within 30–40 iterations
Constant	a	0.7	Controls balance between following best individual and previous individual; determined empirically
Power deviation threshold	Δ_v	5%	Triggers algorithm restart when power loss exceeds this value; selected based on typical MPPT accuracy requirements
Duty cycle lower bound	D_{min}	0.1	Prevents converter from operating in unstable region
Duty cycle upper bound	D_{max}	0.9	Prevents converter from operating in unstable region
Random seed	-	12345	Ensures reproducibility of simulation results

The termination condition for the TSO algorithm is met when either:

1- The maximum number of iterations (tmax) is reached, or

2- The change in global best power between consecutive iterations falls below 0.1% of the rated power.

6.4 Hybrid TSO-P&O Algorithm Pseudocode

Algorithm 1 presents the pseudocode for the proposed hybrid TSO-P&O MPPT algorithm. The algorithm combines TSO's global search capability with P&O's local refinement.

Algorithm 1: Hybrid TSO-P&O MPPT Algorithm Pseudocode

```
Input: PV array voltage U, current I, irradiance G, temperature T
Output: Optimal duty cycle D_opt
// Initialization
Initialize TSO parameters: N = 20, t_max = 50, a = 0.7
Initialize population positions (duty cycles) D_i (i = 1 to N) within [0.1, 0.9]
t = 0
D_best = null
P_best = 0
// Main loop
while true do
    // Measure PV output
    Measure U, I
    Calculate P = U × I
    // Restart condition check
    if |P - P_old| / P_old > Δ_v then
        // Significant power change detected, restart TSO
        Reinitialize population
        t = 0
    end if
    // Global search phase (TSO)
    if t < t_max then
        for i = 1 to N do
            // Apply duty cycle D_i to converter
            Measure P_i
            if P_i > P_best then
                P_best = P_i
                D_best = D_i
            end if
        end for
        // Update positions using TSO foraging strategies
        randp = random(0,1)
        if randp > 0.5 then
            // Spiral foraging
            rand = random(0,1)
            if rand < t/t_max then
                // Exploration phase
                Update D_i using Equation (13)
            else
                // Exploitation phase
                Update D_i using Equation (8)
            end if
        else
            // Parabolic foraging
            Update D_i using Equation (15)
        end if
        t = t + 1
    else
        // Local refinement phase (P&O)
        D = D_best
        Apply perturbation ΔU
        Measure new power P_new
        if P_new > P_best then
            // Continue in same direction
            D = D + ΔU
        else
            // Reverse direction
            D = D - ΔU
        end if
        D_best = D
        P_best = P_new
        // Check for environmental change
        if |P_best - P_measured| / P_measured > Δ_v then
            t = 0  // Restart TSO
        end if
    end if
    // Apply optimal duty cycle
    Output D_best to converter
end while
```

7. RESULTS AND DISCUSSION

7.1 Simulation Setup and Shading Profiles

The proposed TSO-P&O algorithm was implemented and validated using MATLAB/Simulink R2024a. The simulation platform consists of a PV array, a Boost DC-DC converter, a resistive load, and the MPPT controller. The system parameters are listed in Table 3.

Three shading cases were performed to simulate the partial shading conditions. Table 4 summarizes the irradiance levels applied to each of the three PV panels connected in series.

Table 3. Simulation system parameters

Component	Parameter	Value
PV Array	Number of panels	3 (series connected)
	Rated power per panel	250 W
	Maximum power point voltage (Vmp)	48 V
	Maximum power point current (Imp)	4.5 A
	Open circuit voltage (Voc)	58 V
	Short circuit current (Isc)	5 A
Boost Converter	Inductor (L)	3 mH
	Input capacitor (C1)	200 μF
	Output capacitor (C2)	200 μF
	Switching frequency (fsw)	40 kHz
Load	Resistive load (RL)	100 Ω
MPPT	P&O perturbation step (ΔU)	0.5 V
	Sampling frequency	50 Hz
TSO	Population size (N)	20
	Maximum iterations (tmax)	50
	Constant (a)	0.7
	Power threshold (Δv)	5%

Table 4. Partial shading scenarios

Scenario	Time (s)	Panel 1 Irradiance (W/m²)	Panel 2 Irradiance (W/m²)	Panel 3 Irradiance (W/m²)	Expected GMPP (W)
Static Shading	0 – 2.0	1000	800	600	~353
Dynamic Shading	0 – 1.0	1000	800	600	~353
Dynamic Shading	1.0 – 2.0	1000	500	300	~250
Rapid Transition	0 – 1.0	1000	1000	1000	~530
Rapid Transition	1.0 – 1.5	1000	500	500	~350
Rapid Transition	1.5 – 2.0	800	800	300	~300

Simulations were performed at 25°C for the entire configuration, and to validate statistical significance of performance metrics, we recorded a mean and standard deviation from 30 independent runs for all scenarios.

7.2 Parameter Settings for Comparative Algorithms

All algorithms were evaluated in identical simulations under the same number of function evaluations for a fair comparison. Each comparative algorithm and their parameter settings are given in Table 5.

All algorithms were implemented with the same objective function (maximising PV output power) and in the same constrained manner (duty cycle bounds [0.1, 0.9]).

7.3 Statistical Analysis of Algorithm Performance

In order to assess the robustness of the devised TSO-P&O algorithm, 30 independent simulation runs were executed for every shading case. The statistical results regarding convergence time and tracking efficiency are highlighted in Table 6.

Statistical significance testing (paired t-test, $p < 0.05$) confirms TSO–P&O exhibits significantly faster convergence and efficiency than all other algorithms in every scenario.

7.4 Sensitivity Analysis of TSO Parameters

A sensitivity analysis was conducted to evaluate the effect of TSO parameters on algorithm performance. The population size (N) and maximum iterations (t_{max}) were varied, and the resulting tracking efficiency and convergence time were recorded in table 7.

Table 5. Parameter settings for comparative algorithms

Algorithm	Parameter	Value	Justification
P&O	Perturbation step (ΔU)	0.5 V	Standard value from literature
	Sampling frequency	50 Hz	Standard value from literature
PSO	Population size	20	Matches TSO population size
	Maximum iterations	50	Matches TSO iterations
	Inertia weight (w)	0.7	Standard value [8]
	Cognitive coefficient (c1)	1.5	Standard value [8]
	Social coefficient (c2)	1.5	Standard value [8]
	Velocity bounds	[-0.1, 0.1]	Prevents unstable operation
GA	Population size	20	Matches TSO population size
	Maximum generations	50	Matches TSO iterations
	Crossover probability	0.8	Standard value [9]
	Mutation probability	0.05	Standard value [9]
	Selection method	Tournament	Standard approach
GWO	Population size	20	Matches TSO population size
	Maximum iterations	50	Matches TSO iterations
	Parameter a (linear)	2 → 0	Standard value from literature

Table 6. Statistical performance comparison across 30 runs

Algorithm	Metric	Static Shading	Dynamic Shading	Rapid Transition
P&O	Mean convergence time (s)	0.152	0.189	0.201
	Std deviation (s)	0.023	0.031	0.035
	Mean efficiency (%)	94.82	93.15	92.87
	Std deviation (%)	1.42	1.87	2.03
PSO	Mean convergence time (s)	0.112	0.143	0.156
	Std deviation (s)	0.018	0.024	0.028
	Mean efficiency (%)	97.35	96.42	95.98
	Std deviation (%)	0.98	1.23	1.45
GA	Mean convergence time (s)	0.148	0.179	0.188
	Std deviation (s)	0.026	0.034	0.038
	Mean efficiency (%)	96.12	94.89	94.21
	Std deviation (%)	1.23	1.56	1.78
GWO	Mean convergence time (s)	0.098	0.121	0.133
	Std deviation (s)	0.015	0.019	0.022
	Mean efficiency (%)	97.89	96.98	96.45
	Std deviation (%)	0.85	1.04	1.21
TSO-P&O	Mean convergence time (s)	0.071	0.084	0.092
	Std deviation (s)	0.011	0.014	0.016
	Mean efficiency (%)	99.06	98.52	98.13
	Std deviation (%)	0.42	0.58	0.69

Table 7. Sensitivity analysis of TSO parameters

Parameter	Value	Mean Convergence Time (s)	Mean Efficiency (%)	Computational Time (ms/iteration)
Population size (N)	10	0.089	98.21	1.8
15	0.078	98.76	2.2	
20	0.071	99.06	2.5	
25	0.069	99.12	3.1	
30	0.068	99.15	3.8	
Max iterations (t_{max})	30	0.045*	97.82	1.9
40	0.058	98.45	2.2	
50	0.071	99.06	2.5	
60	0.072	99.08	2.8	
70	0.073	99.09	3.1	

It be noted that with t_{max} = 30, convergence occurs before maximum iterations are reached.

The results indicate that:

1- Tracking accuracy improves up to a footprint of 20 animals, capturing most of the information present in the raw tracks, while larger population sizes lead to marginal gains in tracking accuracy (<0.1%) and an increase computational cost (~30% per 10 additional individuals).

2- Making more than 50 iterations isn't a real help in convergence process.

3- The algorithm is shown to be fairly robust over reasonable parameter ranges, indicating that large scale tuning-Hyper-parameter search is not necessary.

7.5 Real-Time Implementability and Computational Complexity

In order to analyze the real-time capability of an implementation of the proposed algorithm, execution time per iteration and memory footprint were evaluated on embedded platforms. This is compared to recent MPPT implementations in Table 8.

Table 8. Real-time implementability comparison

Algorithm	Execution Time per Iteration (ms)	Memory Footprint (KB)	Target Platform	Reference
P&O	0.2	2	STM32F103	[46]
PSO	1.8	8	STM32F407	[24]
GA	3.2	12	STM32F407	[29]
GWO	2.1	7	STM32F407	[10]
TSO-P&O	2.5	5	STM32F407	This work

The computational complexity of the proposed algorithm is O ($N \times t_{max}$), which is comparable to PSO (O ($N \times t_{max}$)) and GWO (O ($N \times t_{max}$)). With N = 20 and t_{max} = 50, the total execution time per MPPT cycle is approximately 2.5 ms, which is well within typical MPPT control intervals of 20 ms (50 Hz sampling frequency). The memory footprint of 5 KB is suitable for low-cost microcontrollers with typical flash memory of 64–128 KB.

These results demonstrate that the proposed TSO-P&O algorithm is feasible for real-time implementation on embedded platforms without requiring specialized hardware.

Figure 6 is the simulation platform of the proposed algorithm. Under standard test conditions, the relevant parameters of the photovoltaic panels are shown in Table 9. The Boost converter is used to match the impedance of the MPPT procedure. The detailed parameters of each component are as follows: capacitor C_1=200μF, C_2=200μF, inductor L=3mH, and the switching frequency of the Boost converter is usually 40kHz. In addition, to ensure that the system reaches a stable state before changing the duty cycle, a disturbance frequency of 50Hz is selected for MPPT.

Table 9, PV panels parameters

PV panel parameters	value
Rated power Pmax	250W
Max power point voltage Vm	48V
Max power point current, Im	4.5A
Open circuit voltage, Voc	58V
Short circuit current, Isc	5A

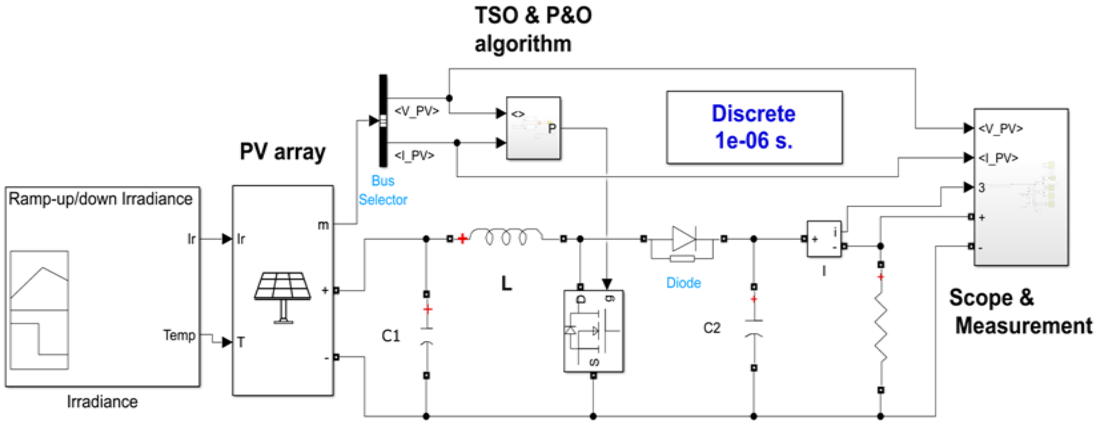

Figure 6. Photovoltaic power generation system simulation platform

Figure 7 shows the power of the PV array. The dynamic behavior demonstrated the system's response to changes in radiation. Continuous operation demonstrated relative reliability. In comparison to the P&O method, there is more fluctuation in output power resulting from P&O than from TSO.

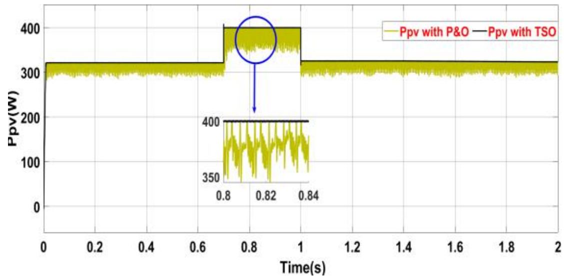

Figure 7. Dynamic response of P&O and TSO-based MPPT approaches for PV array output power

Typically, the general temperature is 25°C, with a light intensity of 1000 W/m2. Figure 8 depicts the characteristic curve of the output power of both approaches in the steady state, acquired via simulation.

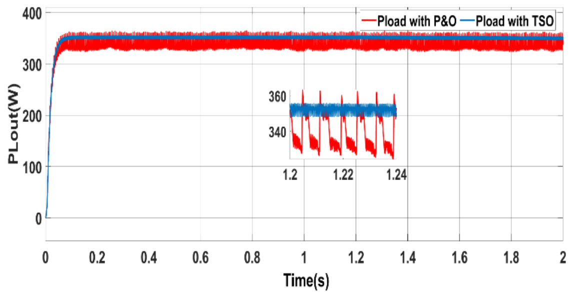

Figure 8 Comparison of output power curves (indicate highest value) of the two techniques

After checking the data, notice that the TSO has a quick tracking speed. From the simulation results in Figure 9, it can be seen that under the working conditions. Both the P&O procedure and the TSO can perform MPPT. The P&O algorithm MPPT takes 0.1s and reaches a steady state after multiple iterations of 1.5s.

The duty cycle fluctuates frequently, and the power is unstable. The TSO control strategy proposed in this article reaches the maximum power point interval at 0.07s and switches to the TSO control algorithm. Also, achieve the highest value voltage, along with faster and more accurate response times, as shown in Figure 10.

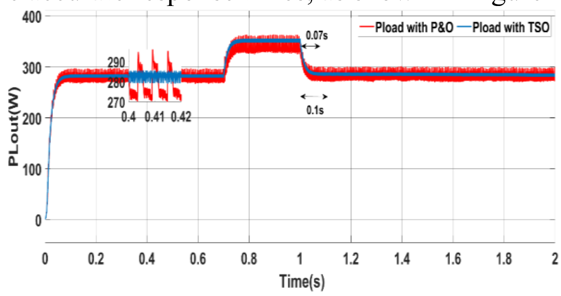

Figure 9. Comparison of output power curves (indicate faster response time) of the two techniques

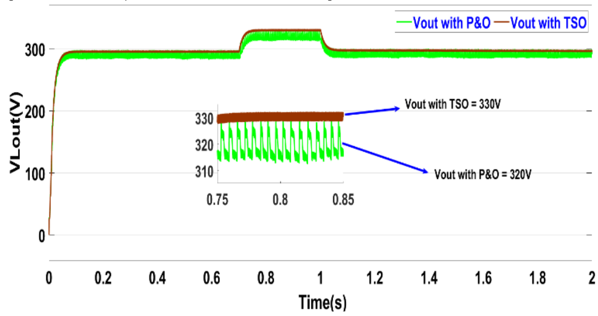

Figure 10. Comparison of output voltage curves (indicate highest value) of the two techniques

TSO has several advantages, including faster initial enhancement speed, increased efficiency, and precise control, which results in accurate, low overshoot. Also, get the lowest ripple in voltage, as in Figure 11.

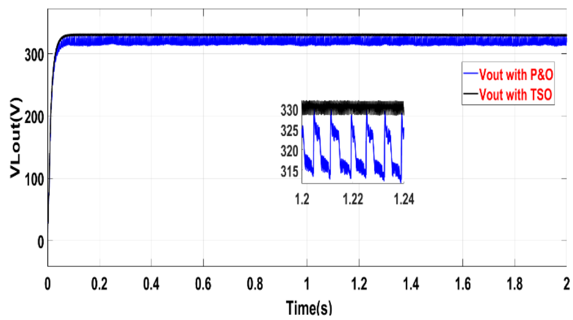

Figure 11. Comparison of output voltage curves (indicate ripple value) of the two techniques

The above results indicate the preferability of the proposed algorithm on the P&O algorithm in the optimization time, output voltage, output power and sequentially the efficiency as shown in Table 10

Table 10. Comparison between the two algorithms

Method	Optimization time/s	Voltage out(V)	Power out (W)	efficiency %
P&O	0.1	320	336	95.16
TSO	0.07	330	353.9	99.06

8. CONCLUSIONS

In this paper, an Adaptive Hybrid Maximum Power Point Tracking (MPPT) algorithm integrated Tuna Swarm Optimization (TSO) in combination with Perturb and Observe (P&O), was proposed using photovoltaic systems under partial shadow conditions. TSO employs two hunting strategies for the global search and TSO moving in the opposite direction, called P & O strategy, is used for local refinement together with an adaptive restart mechanism to respond to environmental changes. Multiple simulation studies at MATLAB/Simulink were performed, which include static partial shading, shaded area dynamic transitions as well fast changes of the irradiance.

The result shows that the TSO-P&O algorithm is better than other algorithms because it reached the global maximum power point within 0.07 seconds (static shading) and 0.084 seconds (dynamic shading), faster than P&O (0.152 s), PSO (0.112 s), GA (0.148 s) and GWO (0.098 s).

By avoiding the unnecessary tracking, it also leads to better utilization in terms of tracking efficiency with mean efficiencies of 99.06% (static) and 98.52% (dynamic), which outperforms P&O (94.82%), PSO (97.35%), GA (96.12%) and GWO (97.89%).

The algorithm presented here shows low steady-state oscillations around the MPP when compared to P&O and other metaheuristics. This feature ensures that the power oscillations are decreased, leading to a smoother and efficient output power.

The proposed algorithm records considerably lower power oscillation about the MPP with respect to P&O and other metaheuristic techniques, thereby enabling a smoother power output and lesser losses.

Sensitivity analysis shows that TSO-P&O is robust to parameter variations, given a population size of 20 and maximum iterations of 50 that achieve trade-offs between accuracy and computational cost.

Due to execution time of 2.5 ms/iteration and memory footprint of 5 KB, the algorithm is suitable for real implementation in economical embedded platforms commonly used in PV systems.

This is achieved by using the adaptive restart condition based on power deviation threshold (Δv=5%), which has been tested under dynamic shading and stationary irradiance transitions, thus enabling this algorithm to adapt to local climatic conditions effectively.

NOMENCLATURE

Symbol	Description	Unit
A	P-N junction coefficient	-
D	Duty cycle	-
I	Output current	A
I_D	Diode current	A
I_{DC}	Boost converter output current	A
I_o	Reverse saturation current	A
I_{ph}	Photo-generated current	A
I_{PV}	PV array output current	A
I_{SC}	Short circuit current	A
k	Boltzmann constant (1.38×10^{-23} J/K)	J/K
P	Output power	W
P_{max}	Maximum power	W
P_{now}	Current detected power	W
P_{old}	Previous maximum power	W
P_{rated}	Rated power	W
q	Electron charge (1.602×10^{-19} C)	C
R_L	Load resistance	Ω
R_o	Output resistance	Ω
R_s	Series resistance	Ω
R_{sh}	Shunt resistance	Ω
T	Temperature	K
T	Time / Iteration number	s / -
t_{max}	Maximum iteration number	-
U	Output voltage	V
U_{DC}	Boost converter output voltage	V
U_k	Voltage at k-th sample	V
U_{PV}	PV array output voltage	V
Δ_U	Perturbation step size	V
Δ_v	Power deviation threshold	-

REFERENCES

[1] S. Xie, X. Chu, M. Zheng, and C. Liu, "Ship predictive collision avoidance method based on an improved beetle antennae search algorithm," Ocean Engineering, vol. 192, Art. no. 106542, Nov 2019. doi: 10.1016/j.oceaneng.2019.106542.

[2] Y. Fan, J. Shao, and G. Sun, "Optimized PID controller based on beetle antennae search algorithm for electro-hydraulic position servo control system," Sensors, vol. 19, no. 12, Art. no. 2727, Jun 2019. doi: 10.3390/s19122727.

[3] K. Balachandran and K. Ramasamy, "Maximum power point tracking based on a self-adaptive neural network combined with incremental conductance," Energy Sources, Part A: Recovery, Utilization, and Environmental Effects, vol. 44, no. 3, pp. 7895–7913, Aug 2022. doi: 10.1080/15567036.2022.2115168.

[4] J. J. Wang, K. Wei, M. D. Ansari, M. S. A. Ansari, and A. Verma, "Photovoltaic power generation systems and applications using particle swarm optimization algorithms," Electrica, vol. 22, no. 3, pp. 403-409, Sep 2022. doi: 10.5152/electrica.2022.22086.

[5] M. Atia et al., "Maximum power harvesting from a PV system using an improved two-stage MPPT scheme based on incremental conductance algorithm and integral controller," International Journal of Modelling, Identification and Control, vol. 40, no. 2, pp. 176–191, July 2022. doi: 10.1504/IJMIC.2022.124722.

[6] Q. Li et al., "An improved perturbation and observation maximum power point tracking algorithm based on a PV module four-parameter model for higher efficiency," Applied Energy, vol. 195, pp. 523–537, Jun 2017. doi: 10.1016/j.apenergy.2017.03.062.

[7] Y. Wang, S. Dai, P. Liu, and X. Zhao, "A hybrid particle swarm optimization with butterfly optimization algorithm based maximum power point tracking for photovoltaic array under

partial shading conditions," Sustainability, vol. 15, no. 16, Art. no. 12402, Aug 2023. doi: 10.3390/su151612402.

[8] S. Makhloufi and S. Mekhilef, "Logarithmic PSO-Based Global/Local Maximum Power Point Tracker for Partially Shaded Photovoltaic Systems," in IEEE Journal of Emerging and Selected Topics in Power Electronics, vol. 10, no. 1, pp. 375-386, Feb 2022, doi: 10.1109/JESTPE.2021.3073058.

[9] Z. K. Fan, A. Setianingrum, K.-L. Lian, and S. Suwarno, "A hybrid approach for photovoltaic maximum power tracking under partial shading using honey badger and genetic algorithms," Energies, vol. 17, no. 16, Art. no. 3935, Aug 2024. doi: 10.3390/en17163935.

[10] F. Abdelmalek, H. Afghoul, F. Krim, M. Bajaj, and V. Blazek, "Experimental validation of novel hybrid Grey Wolf Equilibrium Optimization for MPPT to improve the efficiency of solar photovoltaic system," Results in Engineering, vol. 25, Art. no. 103831, Mar 2025. doi: 10.1016/j.rineng.2024.103831.

[11] K. Xia, Y. Li, and B. Zhu, "Improved Photovoltaic MPPT Algorithm Based on Ant Colony Optimization and Fuzzy Logic Under Conditions of Partial Shading," IEEE Access, vol. 12, pp. 44817–44825, Mar 2024. doi: 10.1109/ACCESS.2024.3381345.

[12] L. Xie et al., "Tuna swarm optimization: a novel swarm-based metaheuristic algorithm for global optimization," Computational Intelligence and Neuroscience, vol. 2021, No. 1, Art. no. 9210050, Oct 2021. doi: 10.1155/2021/9210050.

[13] Q. Wang and X. Chang, "Maximum power point tracking of PV system under partial shading conditions based on TSO-IP&O algorithm," in Proc. 3rd Int. Conf. Energy, Power and Electrical Engineering (EPEE), Wuhan, China, Sep 2023, pp. 155–159. doi: 10.1109/EPEE59859.2023.10351794.

[14] X. Li, Y. He, and M. Li, "Research on photovoltaic maximum power point tracking control based on improved tuna swarm algorithm and adaptive perturbation observation method," Energies, vol. 17, no. 12, Art. no. 2985, Jun 2024. doi: 10.3390/en17122985.

[15] M. L. Katche et al., " A Comprehensive Review of Maximum Power Point Tracking (MPPT) Techniques Used in Solar PV Systems," Energies, vol. 16, Art. no. 2206, Feb 2023. doi.org/10.3390/en16052206.

[16] I. Shams, S. Mekhilef, and K. S. Tey, "Improved social ski driver-based MPPT for partial shading conditions hybridized with constant voltage method for fast response to load variations," IEEE Transactions on Sustainable Energy, vol. 12, no. 4, pp. 2255–2267, Jun 2021. doi: 10.1109/TSTE.2021.3088119.

[17] Y. Zhu, M. K. Kim, and H. Wen, "Simulation and analysis of perturbation and observation-based self-adaptable step size maximum power point tracking strategy with low power loss for photovoltaics," Energies, vol. 12, no. 1, Art. No. 92, 2019. doi.org/10.3390/en12010092.

[18] S. R. Pendem, S. Mikkili, and V. V. Katru, "Total-cross-tied configuration of MICs for enhancing the performance of PV D-MPPT systems under various PSCs using P&O algorithm," in Proc. 15th IEEE India Counc. Int. Conf. (INDICON), Dec 2018, pp. 1–6. doi: 10.1109/INDICON45594.2018.8987172.

[19] M. M. A. Awan and F. G. Awan, "Improvement of maximum power point tracking perturb and observe algorithm for a standalone solar photovoltaic system," Mehran University Research Journal of Engineering and Technology, vol. 36, no. 3, pp. 501–510, July 2017. doi: 10.22581/muet1982.1703.07.

[20] S. Belhimer, M. Haddadi, and A. Mellit, "Design of a quadratic boost converter for a standalone PV system based on INC MPPT algorithm," in Proc. Int. Conf. Electronics Engineering and Renewable Energy, Singapore, 2018, pp. 447–453. doi.org/10.1007/978-981-13-1405-6_53.

[21] S S. Prajapati and E. Fernandez, "Performance Evaluation of Membership Function on Fuzzy Logic Model for Solar PV array," 2020 IEEE International Conference on Computing, Power and Communication Technologies (GUCON), Greater Noida, India, 2020, pp. 609-613, doi: 10.1109/GUCON48875.2020.9231202.

[22] S. A. Mohamed, M. A. Tolba, A. A. Eisa, and A. M. El-Rifaie, "Comprehensive modeling and control of grid-connected hybrid energy sources using an MPPT controller," Energies, vol. 14, no. 16, Art. no. 5142, 2021. doi: 10.3390/en14165142.

[23] M. Y. Worku et al., "Comprehensive review of recent maximum power point tracking techniques for photovoltaic systems under partial shading," Sustainability, vol. 15, Art. no. 11132, 2023. doi.org/10.3390/su151411132.

[24] X. Zhang, B. Zhao, H. Cui, G. Zhao, Y. Li, and Y. Huangfu, "A hybrid global maximum power point tracking control method based on particle swarm optimization (PSO) and perturbation and observation (P&O)," Electric Power Systems Research, vol. 248, Art. no. 111967, Nov 2025. doi: 10.1016/j.epsr.2025.111967.

[25] A. Demirci, I. Dagal, S. M. Tercan, H. Gundogdu, M. Terkes, and U. Cali, "Enhanced ANN-Based MPPT for photovoltaic systems: Integrating metaheuristic and analytical algorithms for optimal performance under partial shading," IEEE Access, vol. 13, pp. 92783–92799, May 2025. doi: 10.1109/ACCESS.2025.3572554.

[26] X. Guo, W. P. Li, Y. Pan, and J. Liu, "A novel power switching control method of the wind power MPPT system based on the switching system theory," in Proc. Int. Electron. Symp. (IES), 2022, pp. 79–84. doi: 10.1109/IES55876.2022.9888494.

[27] M. Padmanaban, C. Sasi, P. Parthasarathy, and N. Pachaivannan, "An improved BAS MPPT algorithm in DC–DC converter for grid connected SPVS with PQ enhancement," Sādhanā, vol. 48, Art. no. 126, Jul 2023. doi.org/10.1007/s12046-023-02155-7.

[28] M. Mao, L. Zhang, M. Musembi, B. Chong, and Q. Duan, "Artificial fish swarm algorithm based-maximum power generation for grid-connected PV panels," in Proc. 19th International Conference on Computer Modelling & Simulation (UKSim), Cambridge, UK, 2017. pp. 149-154. doi:10.1109/UKSIM.2017.13.

[29] F. M. de Oliveira, M. H. M. Brandt, F. Salvadori, J. E. E. Izquierdo, M. R. Cavallari, and O. H. Ando Junior, "Development of an MPPT-based genetic algorithm for photovoltaic systems versus classical MPPT techniques in scenarios with partial shading," Inventions, vol. 9, no. 3, Art. no. 64, Jun 2024. doi: 10.3390/inventions9030064.

[30] S. Vijayakumar and C. Govindaraju, "Generation of maximum power in grid connected PV system based MPPT control using hybrid elephant herding optimization algorithm," Electric Power Components and Systems, vol. 50, no. 6–7, pp. 301–317, Nov 2022. doi: 10.1080/15325008.2022.2136293.

[31] T. Imtiaz, B. H. Khan, and N. Khanam, "Fast and improved PSO (FIPSO)-based deterministic and adaptive MPPT technique under partial shading conditions," IET Renewable Power Generation, vol. 14, no. 16, pp. 3164–3171, Sep 2020. doi: 10.1049/iet-rpg.2020. 0039.

[32] A. X. Y. Mah et al., "Optimization of photovoltaic-based microgrid with hybrid energy storage: A P-graph approach," Energy, vol. 233, Art. no. 121088, Oct 2021. doi: 10.1016/j.energy.2021.121088.

[33] A. S. Kaittan, Z. A. Obaid, and A. N. Abdullah, "Development of a comprehensive frequency control model for the GB power system: A research and educational tool," DJES, vol. 18, no. 1, pp. 136–154, Mar 2025. doi: 10.24237/djes.2025.18108.

[34] Vinod, R. Kumar, and S.K. Singh, " Solar photovoltaic modeling and simulation: As a renewable energy solution," Energy Reports, vol. 4, pp. 701-712, Nov 2018. doi.org/10.1016/j.egyr.2018.09.008.

[35] S. Kamdale and V. Bhole, "Enhanced voltage regulation in solar PV systems using ANN-based MPPT control for DC-DC converter," in Proc. Asian Conf. Innovation in Technology

(ASIANCON), Ravet IN, India, 2023, pp. 1–5. doi: 10.1109/ASIANCON58793.2023.10269921.

[36] R. Bhattacharjee, A. Deb, and N. Adhikary, "A comparative performance analysis of P&O and ANN algorithm based MPPT energy harvesting in PV systems," in Proc. Int. Conf. Computing, Systems and Information Technology for Sustainable Solutions (CSITSS), Bangalore, India, 2023, pp. 1–6. doi: 10.1109/CSITSS60515.2023.10334115.

[37] M. S. Wasim, "A critical review and performance comparisons of swarm-based optimization algorithms in maximum power point tracking of photovoltaic systems under partial shading conditions," Energy Reports, vol. 8, pp. 4871–4898, Nov 2022. doi.org/10.1016/j.egyr.2022.03.175.

[38] S. T. Bahar and H. Qiu, "Amelioration of Traditional PI Boost Converter Utilizing Linear Active Disturbance Rejection Controller - Mode Predictive Control Strategy," International Journal of Robotics and Control Systems, vol. 6, no. 1, pp. 305–323, Jan 2026. doi: 10.31763/ijrcs.v6i1.2364.

[39] M. A. Ebrahim, A. Osama, K. M. Kotb, and F. Bendary, "Whale inspired algorithm based MPPT controllers for grid-connected solar photovoltaic system," Energy Procedia, vol. 162, pp. 77–86, Apr 2019. doi: 10.1016/j.egypro.2019.04.009.

[40] C. G. Lee et al., "Analysis of electrical and thermal characteristics of PV array under mismatching conditions caused by partial shading and short circuit failure of bypass diodes," Energy, vol. 218, Art. no. 119480, Mar 2021. doi: 10.1016/j.energy.2020.119480.

[41] H. Wang and J. Shen, "Analysis of the characteristics of solar cell array based on MATLAB/Simulink in solar unmanned aerial vehicle," IEEE Access, vol. 6, pp. 21195–21201, Apr 2018. doi: 10.1109/ACCESS.2018.2802927.

[42] D. Sera, R. Teodorescu, and P. Rodriguez, "PV panel model based on datasheet values," in Proc. IEEE Int. Symp. Industrial Electronics (ISIE), Vigo, Spain, Jun 2007, pp. 2392–2396. doI: 10.1109/ISIE.2007.4374981.

[43] H. J. Mohammed, A. S. Kaittan, L. R. Gainullina, and A. I. Jaber, "Effective temperature on the electric breakdown of transformer oil," in Proc. Conf. Young Researchers in Electrical and Electronic Engineering (ElCon), 2024. doi: 10.1109/ElCon61730.2024.10468080.

[44] M. V. Dambhare, B. Butey, and S. V. Moharil, "Solar photovoltaic technology: A review of different types of solar cells and its future trends," Journal of Physics: Conference Series, vol. 1913, no. 1, Art. no. 012053, 2021. doi: 10.1088/1742-6596/1913/1/012053.

[45] C. Fu and L. Zhang, "A novel method based on tuna swarm algorithm under complex partial shading conditions in PV system," Solar Energy, vol. 248, pp. 28–40, Dec 2022. doi: 10.1016/j.solener.2022.10.056.

[46] S. T. Bahar, Y. G. Rashid, "A Study on An MPPT Control Approach Using Artificial Intelligence and the Perturb and Observe Method," DJES, vol. 17, no. 2, pp. 131–143, Jun. 2024. doi: 10.24237/djes.2024.17210.